An Optimal Direct Synthesis of CrSBA-15 Mesoporous Materials with Enhanced Hydrothermal Stability

M. Selvaraj and S. Kawi*

Department of Chemical & Biomolecular Engineering, National University of Singapore, Singapore 119260

Received August 25, 2006. Revised Manuscript Received October 19, 2006

Mesoporous CrSBA-15 materials with different n_{Si}/n_{Cr} ratios have been synthesized, for the first time, using Pluronic P123 as a structure-directing agent by simply adjusting the molar ratio of water to hydrochloric acid (n_{H_2O}/n_{HCl}). The effect of the nature of Cr-ion source on the synthesis of CrSBA-15 has been investigated using different chromium-ion sources: chromium(III) nitrate, chromium(III) chloride, and chromium(III) sulfate. To investigate the effect of structural and textural properties with a higher Cr incorporation, CrSBA-15 has also been synthesized with various n_{Si}/n_{Cr} ratios and synthesis temperatures. The synthesized CrSBA-15 materials have been characterized by ICP-AES, XRD, N_2 adsorption, ESR, TEM, and FE-SEM. ICP-AES results show that chromium(III) nitrate nonohydrate is found to be a good Cr-ion source for the synthesis of mesoporous CrSBA-15 material, with a n_{Si}/n_{Cr} ratio up to 9.1 successfully prepared by changing the n_{Si}/n_{Cr} ratio in the synthesis gel at a n_{H_2O}/n_{HCl} of 295. For all calcined CrSBA-15 materials, XRD reflection peaks shift to lower angle with increasing Cr-content, resulting in the increase of the unit cell parameter. By increasing the crystallization temperature from 373 to 403 K, nitrogen adsorption measurement shows that the pore diameter of CrSBA-15 can be tuned from 89.4 to 94.7 Å, with an increase of pore volume from 1.10 to 1.20 cm^3/g accompanied by the concomitant decrease of surface area from 987 to 797 m^2/g and the decrease of pore wall thickness from 38 to 36.7 Å. ESR measurements show the amount of Cr-ions incorporated, as well as the location and coordination of Cr-ion on SBA-15 silica walls. TEM and FE-SEM images show the uniform pore diameter and ropelike hexagonal mesoporous structure of CrSBA-15. Furthermore, the hydrothermal stability of CrSBA-15 samples has also been investigated, with hexagonal CrSBA-15(8) having better hydrothermal stability than CrSBA-15(50).

Introduction

The discovery of highly ordered mesoporous silicate materials with high surface area, large pore size, and large pore volume has attracted great interest for their potentially wide applications, such as in catalysis, adsorption, separation, and ion exchange.[1,2] Up to now, a variety of highly ordered mesoporous silica materials (such as M41S,[1,2] SBA,[3,4] MSU,[5] FDU,[6,7] HMS,[8,9] and KIT[10]) have been successfully synthesized. Although MCM-41 and MCM-48 materials offer great advantages for the adsorption and conversion of bulky molecules in the studies of adsorption, catalysis, and drug delivery systems, pure mesoporous silica materials have not been used as catalysts or catalyst supports in industry yet due to the lack of acidity and poor hydrothermal stability. Furthermore, these mesoporous materials are easily destroyed in boiling water and steam as a result of the fast hydrolysis of the relatively thin amorphous silica pore walls.[10−13]

Highly tailored mesoporous inorganic composite materials have been widely used in catalysis research. The incorporation of transition-metal elements such as Al, Fe, Ga, Mn, Cr, Zr, or V into the amorphous silica walls is mandatory for the formation of catalytically active sites in mesoporous molecular sieves.[14−16] Depending on the type of transition-

* To whom correspondence should be addressed. Tel.: +65-65166312. Fax: +65- 67791936. E-mail: chekawis@nus.edu.sg.

(1) Kresge, C. T.; Leonowicz, M. E.; Roth, W. J.; Vartuli, J. C.; Beck, J. S. *Nature* **1992**, *359*, 710.
(2) Beck, J. S.; Vartuli, J. C.; Roth, W. J.; Leonowicz, M. E.; Kresge, C. T.; Schmitt, K. D.; Chu, C. T. W.; Olson, D. H.; Sheppard, E. W.; McCullen, S. B.; Higgins, J. B.; Schlenker, J. L. *J. Am. Chem. Soc.* **1992**, *114*, 10834.
(3) Zhao, D. Y.; Feng, J. L.; Huo, Q. S.; Melosh, N.; Fredrickson, G. H.; Chmelka, B. F.; Stucky, G. D. *Science* **1998**, *279*, 548.
(4) Zhao, D. Y.; Huo, Q. S.; Feng, J. L.; Chmelka, B. F.; Stucky, G. D. *J. Am. Chem. Soc.* **1998**, *120*, 6024.
(5) Bagshaw, S. A.; Prouzet, E.; Pinnavaia, T. J. *Science* **1995**, *269*, 1242.
(6) Liu, X. Y.; Tian, B. Z.; Yu, C. Z.; Gao, F.; Xie, S. H.; Tu, B.; Che, R. C.; Peng, L. M.; Zhao, D. Y. *Angew. Chem., Int. Ed.* **2002**, *41*, 3876.
(7) Yu, C. Z.; Tian, B. Z.; Fan, B.; Stucky, G. D.; Zhao, D. Y. *Chem. Commun.* **2001**, 2726.
(8) Tanev, P. T.; Pinnavaia, T. J. *Science* **1995**, *267*, 865.
(9) Tanev, P. T.; Chibwe, M.; Pinnavaia, T. J. *Nature* **1994**, *368*, 321.
(10) Ryoo, R.; Kim, J. M.; Ko, C. H.; Shin, C. H. *J. Phys. Chem.* **1996**, *100*, 17718.
(11) Van Der Voort, P.; Baltes, M.; Vansant, E. F. *Catal. Today* **2001**, *68*, 119.
(12) Kawi, S.; Shen, S. C. *Mater. Lett.* **2000**, *42*, 108.
(13) Ryoo, R.; Jun, S. *J. Phys. Chem. B* **1997**, *101*, 317.
(14) Flanigen, E. M.; Lok, B. M.; Patton, R. L.; Wilson, S. T. U.S. Patent 738,887, 1988.
(15) (a) Chen, J.; Dakka, J.; Sheldon, R. *Appl. Catal., A* **1994**, *108*, L1. (b) Chen, J.; Haanepen, M.; van Hooff, J.; Sheldon, R. In *Zeolites and Related Microporous Materials State of the Art*; Weitkamp, J., Karge, H. G., Pfeifer, H., Holderich, W., Eds.; Elsevier: Amsterdam, 1994; p 973 [*Stud. Surf. Sci. Catal.* **1994**, *84*, 973]. (c) Chen, J. D.; Sheldon, R. A. *J. Catal.* **1995**, *153*, 1. (d) Chen, J. D.; Lempers, E. B.; Sheldon, R. *J. Chem. Soc., Faraday Trans.* **1996**, *92*, 1807.
(16) (a) Corma, A. *Chem. Rev.* **1997**, *97*, 2373. (b) Ying, Y. J.; Mehnert, C. P.; Wong, M. S. *Angew. Chem., Int. Ed.* **1999**, *38*, 56.

10.1021/cm062009r CCC: $37.00
Published on Web 01/09/2007

metal species, the coordination, and the number of metal species incorporated in the framework of silica walls, both the Bronsted and Lewis acid sites and their strength might be varied. Generally, mesoporous materials have lower content of acid sites as compared to zeolites. Because of its uniform pore size, mesoporous M-MCM-41 (where M stands for transition metal) is a promising catalyst in most chemical industries to synthesize bulky fine chemicals. For instance, CrMCM-41 catalysts have been used for a variety of reactions such as oxidation of aromatics[17−19] and dehydrogenation of lower alkane.[20]

Mesoporous MSBA-15 has been tested recently as a potential catalyst because MSBA-15 has more advantages than MMCM-41, such as better hydrothermal stability, due to pore walls that are thicker than those of MMCM-41.[1,27] Several researchers reported the incorporation of heteroatoms such as Al,[22] Fe,[23] V,[24] Ti,[25] and Ga[26] in the framework of SBA-15 by direct synthesis or postsynthetic grafting method to create active sites on the silica surface, and these materials have been tested for their catalytic activities for a certain reaction. The procedure of direct-synthesis of MSBA-15 is relatively simple. For example, Yue et al.[22] synthesized AlSBA-15 at a pH value of 1.5, Zhang et al.[25] prepared TiSBA-15 by controlling the hydrolysis of the siliceous source in the presence of fluoride, Newalkar et al.[27] prepared TiSBA-15 under microwave hydrothermal conditions, and Yang et al.[21,28] prepared mesoporous aluminosilicates and titanosilicates in nonaqueous media. However, the efficiency of direct-synthesis is always low because only a small portion of the heteroatoms added into the initial gels can be introduced into the framework of mesoporous materials in aqueous solution. Postsynthesis-grafting procedures have also been performed for mesoporous materials prepared under acidic conditions. For example, Luan et al.[29] synthesized AlSBA-15 by postsynthesis modification either with aluminum isopropoxide in dry hexane, with $AlCl_3$ in dry ethanol, or with an aqueous solution of sodium aluminate. Luan et al. also prepared TiSBA-15[30] and VSBA-15[24] by incipient-wetness impregnation inside a glovebox under flowing nitrogen. Morey et al.[31] synthesized both TiMCM-48 and TiSBA-15 by reacting titanium isopropoxide with dehydrated mesoporous materials in dry hexane media in a Schlenk line under the protection of argon. Although postsynthesis can introduce more heteroatoms into mesoporous silica as compared to direct-synthesis, the postsynthesis routes mentioned above are all relatively complicated, and in some cases the process has to be carried out under conditions that do not include water and oxygen.[24,29,30] Another disadvantage of postsynthesis is that the uniform mesostructure is sometimes severely destroyed.[29] Moreover, it is also difficult to incorporate heteroatoms quantitatively into the materials by postsynthesis because the grafting procedures are mostly processed by immersing solid mesoporous silica into an aqueous or nonaqueous solution followed by filtration and calcination, and heteroatoms may be partially leached out during filtration. Additionally, not all heteroatoms introduced by postsynthesis could be located at the mesoporous walls in 4-coordinated environments, and there are always 6-coordinated heteroatom species in the resultant materials.[24,29,30,32−34] To avoid the above disadvantages, Melero et al., Wu et al., and Li et al. reported,[35] for the first time, that the Ti^{4+} and Al^{3+} species were highly substituted into mesoporous SBA-15 molecular sieves by the "pH-adjusting" method in synthesis gel. However, to the best of our knowledge, the effect of different Cr sources and crystallization temperature under direct hydrothermal synthesis to incorporate a higher amount of Cr-ion in the framework of SBA-15 along with enhanced hydrothermal stability has not been clearly reported in the open literature so far.

In the present study, we report, for the first time, an effective and convenient synthesis procedure to prepare mesoporous CrSBA-15 molecular sieves with very high Cr loadings simply by adjusting the molar ratio of n_{H_2O}/n_{HCl} (pH > 2) under direct hydrothermal conditions. The effect of the nature of Cr-ion source on the synthesis of CrSBA-15 has also been investigated by using different chromium-ion sources, chromium(III) nitrate, chromium(III) chloride, and chromium(III) sulfate. The effect of synthesis temperature of CrSBA-15 under fixed molar ratios of $n_{Si}/n_{Cr} = 8$ and $n_{H_2O}/n_{HCl} = 295$ in the synthesis gel has also been investigated. CrSBA-15 materials have also been treated in steam and boiling water to show their good hydrothermal and thermal stabilities.

Experimental Section

1. Chemicals. All chemicals, triblock copolymer poly(ethylene glycol)-*block*-poly(propylene glycol)-*block*-poly(ethylene glycol) (Pluronic P123, molecular weight = 5800, $EO_{20}PO_{70}EO_{20}$), tetra-

(17) Ulagappan, N.; Rao, C. N. R. *Chem. Commun.* **1996**, 1047.
(18) Zhu, Z.; Chang, Z.; Kevan, L. *J. Phys. Chem. B* **1999**, *103*, 2680.
(19) Sakthivel, A.; Selvam, P. *J. Catal.* **2002**, *211*, 134.
(20) Takehira, K.; Ohishi, Y.; Shishido, T.; Kawabata, T.; Takaki, K.; Zhang, Q.; Wang, Y. *J. Catal.* **2004**, *224*, 404.
(21) Yang, P.; Zhao, D.; Margolese, D.; Chmelka, B. F.; Stucky, G. D. *Nature (London)* **1998**, *396*, 152.
(22) (a) Yue, Y.; Gideon, A.; Bonardet, J.-L.; Melosh, N.; D'Espinose, J.-B.; Fraissard, J. *Chem. Commun.* **1999**, 1967. (b) Vinu, A.; Murugesan, V.; Bohlmann, W.; Hartmann, M. *J. Phys. Chem. B.* **2004**, *108*, 11496.
(23) Nozaki, C.; Lugmair, C. G.; Bell, A. T.; Tilley, T. D. *J. Am. Chem. Soc.* **2002**, *124*, 13194.
(24) Luan, Z.; Bae, J. Y.; Kevan, L. *Chem. Mater.* **2000**, *12*, 3202.
(25) Zhang, W. H.; Lu, J.; Han, B.; Li, M.; Xiu, J.; Ying, P.; Li, C. *Chem. Mater.* **2002**, *14*, 3413.
(26) Berrichi, Z. E.; Cherif, L.; Orsen, O.; Fraissard, J.; Tessonnier, J.-P.; Vanhaecke, E.; Louis, B.; Ledoux, M. J.; Huu, C. P. *Appl. Catal., A* **2006**, *298*, 194.
(27) Newalkar, B. L.; Olanrewaju, J.; Komarneni, S. *Chem. Mater.* **2001**, *13*, 552.
(28) Yang, P.; Zhao, D.; Margolese, D.; Chmelka, B.; Stucky, G. D. *Chem. Mater.* **1999**, *11*, 2813.
(29) Luan, Z.; Hartmann, M.; Zhao, D.; Zhou, W.; Kevan, L. *Chem. Mater.* **1999**, *11*, 1621.
(30) Luan, Z.; Maes, E. M.; van der Heide, P. A. W.; Zhao, D.; Czernuszewicz, R. S.; Kevan, L. *Chem. Mater.* **1999**, *11*, 3680.
(31) Morey, M.; O'Brien, S.; Schwarz, S.; Stucky, G. D. *Chem. Mater.* **2000**, *12*, 898−911.
(32) Mokaya, R. *Angew. Chem.* **1999**, *111*, 3079; *Angew. Chem., Int. Ed.* **1999**, *38*, 2930.
(33) Ryoo, R.; Jun, S.; Kim, J. M.; Kim, M. J. *Chem. Commun.* **1997**, 2225.
(34) Sumiya, S.; Oumi, Y.; Uozumi, T.; Sano, T. *J. Mater. Chem.* **2001**, *11*, 1111.
(35) (a) Melero, J. A.; Arsuaga, J. M.; Frutos, P. D.; Iglesias, J.; Sainz, J.; Blazquez, S. *Microporous Mesoporous Mater.* **2005**, *86*, 364. (b) Wu, S.; Han, Y.; Zou, Y. C.; Song, J. W.; Zhao, L.; Di, Y.; Liu, S. Z.; Xiao, F. S. *Chem. Mater.* **2004**, *16*, 486. (c) Li, Y.; Zhang, L.; Yang, Q.; Wei, Z.; Feng, Z.; Li, C. *J. Phys. Chem. B* **2004**, *108*, 9739.

ethyl orthosilicate (TEOS), hydrochloric acid (HCl), Cr(III) nitrate nonohydrate (99.99+%), Cr(III) chloride hexahydrate (98.0%), and Cr(III) sulfate hydrate (99.999%), were purchased from Aldrich Chemical Inc. All chemicals were used as received without further purification. Millipore water was used in all experiments.

2. Synthesis. Mesoporous CrSBA-15 molecular sieve materials were synthesized using a Pluronic P123 as a structure-directing agent. In a typical synthesis, 4 g of Pluronic P123 was added to 25 mL of water to get a clear solution. Thereafter, a required amount of dilute HCl solution was added, and the solution was again stirred for another 1 h for the hydronium ions to be associated with the alkylene oxide units. Next, 9 g of tetraethyl orthosilicate and a required amount of the desired Cr source were added, and the resulting mixture was stirred for 24 h at 313 K. A first set of samples was prepared by changing the molar water to hydrochloric acid ratio, denoted as CrSBA-15(*x*H), where *x* denotes the molar water to hydrochloric acid ratio (n_{H_2O}/n_{HCl}). For this set of samples, the n_{Si}/n_{Cr} ratio in the gel was fixed to 8. A second set of samples was prepared using different Cr sources by fixing the molar water to hydrochloric acid ratio at 295 (70 mL of 0.29 M HCl) and the n_{Si}/n_{Cr} ratio at 6. These samples are denoted as CrSBA-15(CN), CrSBA-15(CC), and CrSBA-15(CS), where CN, CC, and CS are the abbreviated forms of Cr(III) nitrate nonohydrate (deep violet crystals), Cr(III) chloride hexahydrate (green crystalline powder), and Cr(III) sulfate hydrate (dark green crystals), respectively. A third set of samples was prepared by changing the molar ratio of n_{Si}/n_{Cr} (n_{Si}/n_{Cr} = 4, 16, 25, and 50) by fixing the molar water to hydrochloric acid ratio at 295 (75 mL of 0.29 M HCl). A fourth set of CrSBA-15 samples was prepared by varying the synthesis temperature from 373 to 403 K by fixing the n_{Si}/n_{Cr} ratio at 8 and the n_{H_2O}/n_{HCl} ratio at 295. The samples are labeled as CrSBA-15-(*y*K), where *y* denotes the synthesis temperature.

All of the solid products prepared above, having the molar gel composition of 1 TEOS/0.02−0.25 Cr_2O_3/0.016 P123/0.43−5.2 HCl/127−210 H_2O, were recovered by filtration, washed several times with water, and dried overnight at 373 K. Finally, the samples were calcined in air at 813 K for 6 h for complete removal of the surfactant template.

3. Evaluation of Hydrothermal Stability. The hydrothermal stability of CrSBA-15 materials was investigated by exposing the samples to pure steam (100% water vapor) at different temperatures or in pure boiling water under various treatment times at autogenous pressure.

4. Characterization. The elemental composition of the resultant solid products was analyzed by ICP-AES (Perkin-Elmer, Optima 3000) after the samples were dissolved in a HF solution. The small-angle XRD patterns were recorded under ambient conditions on a Shimadzu XRD-6000 with Cu Kα radiation (λ = 1.5406 Å). The X-ray tube was operated at 40 kV and 30 mA while the diffractograms were recorded in the 2θ range of 0.6−10° with a 2θ step size of 0.01 and a step time of 10 s. Nitrogen adsorption/desorption measurements were conducted using Quantachrome Autosorb-1 by N_2 physisorption at 77 K. All samples were outgassed for 3 h at 250 °C under vacuum ($p < 10^{-5}$ hPa) in the degas port of the sorption analyzer. The BET specific surface areas of the samples were calculated in the range of relative pressures between 0.05 and 0.35. The pore size distributions were calculated from the adsorption branch of the isotherm using the thermodynamics-based Barrett−Joyner−Halenda (BJH) method. The total pore volume was determined from the adsorption branch of the N_2 isotherm at P/P_0 = 1. ESR spectra of the as-synthesized and calcined samples were recorded at the X-band at 298 K on a Bruker ESP 300 spectrometer. The magnetic field was calibrated with a Varian E-500 gaussmeter, and the microwave frequency was measured by an HP 5342A frequency counter. Field-emission scanning electron microscopy (FESEM) images were obtained with a JEOL JSM-6700F microscope at an accelerating voltage of 5.0 kV. Transmission electron microscopy (TEM) images were collected on a JEOL 2010 electron microscope operated at an acceleration voltage of 200 kV.

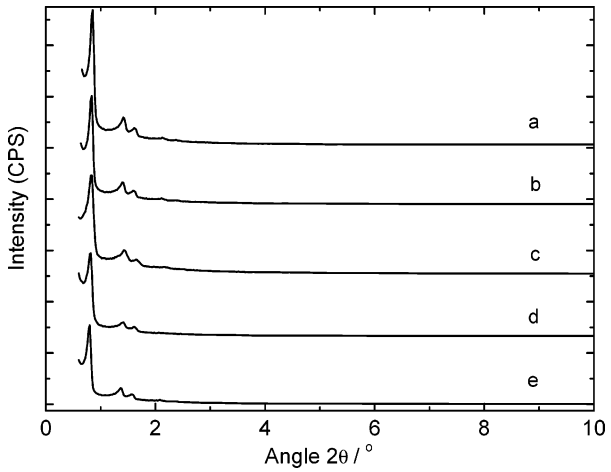

Figure 1. XRD powder patterns of CrSBA-15 materials prepared at different n_{H_2O}/n_{HCl} ratios: (a) SiSBA-15(40H), (b) CrSBA-15(40H), (c) CrSBA-15(70H), (d) CrSBA-15(166H), and (e) CrSBA-15(295H).

Results and Discussion

Effect of n_{H_2O}/n_{HCl} Molar Ratios. Because mesoporous pure silica SBA-15 materials were synthesized under strongly acidic hydrothermal conditions (under $n_{H_2O}/n_{HCl} < 40$, or pH < 1), it is difficult to synthesize Cr-incorporated SBA-15 with a high amount of Cr loading because the Cr−O−Si bonds are easily dissociated due to the hydrolysis of Cr precursors with silicon precursors. However, by decreasing the acidity of the solution (i.e., by increasing the n_{H_2O}/n_{HCl} ratio) to decrease the hydrolysis rate of the Cr precursors to match that of the silicon precursors, the interaction between the Cr−OH and Si−OH species in the synthesis gel could be enhanced, resulting in a higher amount of Cr-ion incorporated in the framework of SBA-15. Therefore, this paper reports a direct synthesis of a higher amount of Cr incorporated in the SBA-15 silica pore walls by simply adjusting the n_{H_2O}/n_{HCl} molar ratio from 40 to 295 in the gel without changing the structural integrity of the parent SBA-15 materials.

The powder XRD patterns of CrSBA-15(*x*H) samples prepared using different water to hydrochloric acid molar ratios (n_{H_2O}/n_{HCl}) are shown in Figure 1. The well-defined XRD patterns are similar to those recorded for all silica SBA-15 materials as described by Zhao et al.[3] The XRD patterns of all CrSBA-15(*x*H) materials exhibit five well-resolved peaks, which are indexed to the (100), (110), (200), (210), and (300) reflections of the hexagonal space group *p*6*mm*, and the XRD peaks are observed to shift to lower angle with increasing Cr-content. The unit cell parameter a_0 is calculated from $a_0 = 2d_{100}/\sqrt{3}$, where the *d*-spacing values are calculated by $n\lambda = 2d \sin\theta$. The observed *d* spacings and unit cell parameter results are well-matched with the hexagonal *p*6*mm* space group. When the n_{H_2O}/n_{HCl} molar ratio is gradually increased from 40 to 295, the size of the unit

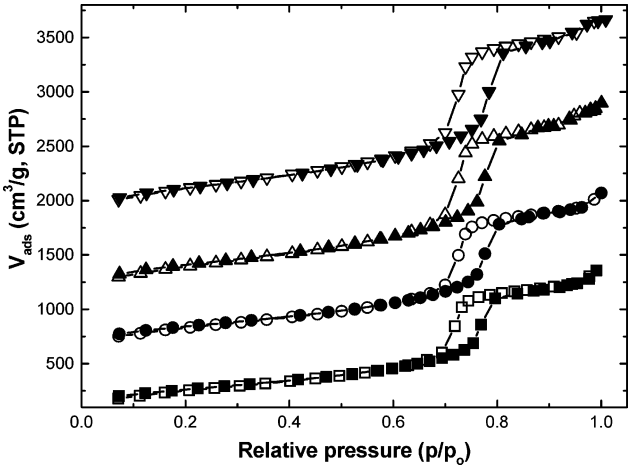

Figure 2. Nitrogen adsorption isotherms of CrSBA-15 materials prepared at different n_{H_2O}/n_{HCl} ratios (closed symbols, adsorption; open symbols, desorption): (■) CrSBA-15(40H), (●) CrSBA-15(70H), (▲) CrSBA-15(166H), and (▼) CrSBA-15(295H).

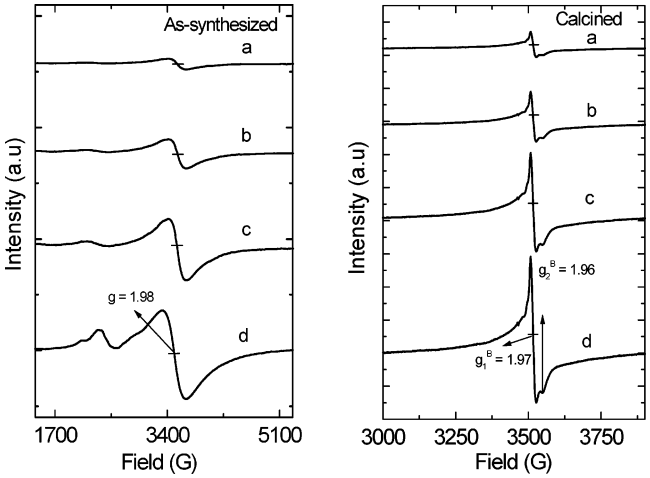

Figure 3. ESR spectra of CrSBA-15 materials prepared at different n_{H_2O}/n_{HCl} ratios: (a) CrSBA-15(40H), (b) CrSBA-15(70H), (c) CrSBA-15(166H), and (d) CrSBA-15(295H).

cell a_0 increases from 118.5 to 127.4 Å due to the increase of Cr-ion incorporated on silica pore walls. This is because the Cr−O bond length is higher than the Si−O bond length due to the larger ionic radius of Cr than Si. Moreover, it is found through ICP-AES analysis that the n_{Si}/n_{Cr} ratio of the calcined CrSBA-15(*x*H) decreases from 162.4 to 9.9 under increasing molar ratio of n_{H_2O}/n_{HCl}. The above-described experimental results suggest that the pH-adjusting method is necessary for a higher amount of Cr-ion incorporation on the silica pore walls without affecting the structural order of the parent SBA-15 materials.

The N_2 adsorption−desorption isotherms and pore size distribution of calcined CrSBA-15(*x*H) prepared under various water to hydrochloric acid molar ratios (n_{H_2O}/n_{HCl}) are shown in Figure 2. The textural properties of CrSBA-15 samples are given in Table 1. All isotherms are of type IV according to the IUPAC classification and exhibited a H1-type broad hysteresis loop, which is typical of large-pore mesoporous solids.[36] As the relative pressure increases ($p/p_0 > 0.6$), all isotherms exhibit a sharp step characteristic of capillary condensation of nitrogen within uniform mesopores, where the p/p_0 position of the inflection point is correlated to the diameter of the mesopore. Because SBA-15 has a hexagonal arrangement of mesopores connected by smaller micropores,[37] it is clear that the broad hysteresis loop observed in the isotherms of CrSBA-15 reflects the long mesopores, which limit the emptying and filling of the accessible volume.

Textural properties such as specific surface area, pore diameter, pore volume, and pore wall thickness of CrSBA-15(*x*H) samples systematically increase with increasing molar ratio of n_{H_2O}/n_{HCl}. CrSBA-15(40H) has a lower surface specific surface area (880 m^2/g), but CrSBA-15(295H) has a higher surface area (999 m^2/g), with the pore volume and pore wall thickness of the corresponding samples increasing from 1.06 to 1.10 cm^3/g and 32.2 to 38 Å, respectively. The pore diameter of CrSBA-15(295H) is 89.4 Å, which is 3.1 Å higher than the sample prepared at very low n_{H_2O}/n_{HCl} ratio of 40 (see Figure 1S in the Supporting Information). It is also interesting to note that the specific surface area, specific pore volume, pore diameter, and pore wall thickness of CrSBA-15(295H) are higher than those of other CrSBA-15(*x*H) and pure silica SBA-15 materials because CrSBA-15(295H) has a higher amount of Cr species than other CrSBA-15(*x*H). Particularly, CrSBA-15 has a higher pore diameter than SiSBA-15 because Cr−O has a higher bond length than Si−O. Based on the above observations, a higher n_{H_2O}/n_{HCl} ratio favors Cr-ion incorporation into SBA-15 without affecting the structural order.

Figure 3 shows the ESR spectra of octahedral Cr^{3+} at $g^A = 1.98$ in as-synthesized CrSBA-15(*x*H) samples. The ESR intensity of octahedral Cr^{3+} in the SBA-15 samples increases because the incorporation of Cr-ions in the silica walls increases with increasing molar n_{H_2O}/n_{HCl} ratio, while the line width systematically increases slightly with Cr-ion content, indicating that Cr-ions are highly incorporated as coordinated tetrahedral Si^{4+} in as-synthesized CrSBA-15. After calcination, the octahedral Cr^{3+} signal disappears while the signal of O_2^- radical with $g_1^B = 1.97$ and $g_2^B = 1.96$, respectively appears (Figure 3). The intensity of the signal of O_2^- radical increases linearly with the amount of Cr-ion incorporated in the framework of CrSBA-15. The signal of O_2^- radical is not observed in calcined siliceous SBA-15(*x*H). The g_3^B value of the O_2^- radical is strongly dependent on the positive charge of the nearest cation.[38] Generally, with an increase of the metal ion oxidation state from 1 to 6, g_2 decreases from about 1.97 to about 1.95. The fact that the intensity of O_2^- radical increases linearly with Cr-ion content and that g_2^B is around 1.96 indicates that the O_2^- radical is connected with the tetrahedral Cr^{6+} species to form $Cr^{6+}-O_2^-$ complex. Based on the ESR spectra characterizing the interaction of tetrahedral Cr^{5+} with O_2, it can be observed that $Cr^{6+}-O_2^-$ in calcined CrSBA-15 is produced as follows. During the calcination of CrSBA-15, octahedral Cr^{3+} is oxidized to tetrahedral Cr^{5+}, which then coordinates with one molecule of O_2 to form a five-coordinated square-pyramidal $Cr^{5+}-$

(36) Sayari, A.; Liu, P.; Kruk, M.; Jaroniec, M. *Langmuir* **1997**, *13*, 2499.
(37) Imperor-Clerc, M.; Davidson, P.; Davidson, A. *J. Am. Chem. Soc.* **2000**, *122*, 11925.
(38) Dyrek, K.; Che, M. *Chem. Rev.* **1997**, *97*, 305.

Table 1. Structural and Textural Parameters of CrSBA-15 Materials Prepared at Different n_{H_2O}/n_{HCl} Ratios

sample	n_{H_2O}/n_{HCl}	n_{Si}/n_{Cr} ratio gel	n_{Si}/n_{Cr} ratio calcined	Cr (wt %)	d_{100} (Å)	a_o (Å)	A_{BET} (m^2/g)	d_p (Å)	V_p (cm^3/g)	$t_w = a_o - d_p$ (Å)
SiSBA-15(40H)	40				102.4	118.2	908	87.4	1.07	30.3
CrSBA-15(40H)	40	8	162.4	0.027	102.6	118.5	880	86.3	1.06	32.2
CrSBA-15(70H)	70	8	78.3	0.055	105.1	121.3	927	87.5	1.07	33.8
CrSBA-15(166H)	166	8	28.5	0.152	107.6	124.2	948	88.3	1.08	35.9
CrSBA-15(295H)	295	8	9.9	0.439	110.3	127.4	999	89.4	1.10	38.0

Scheme 1

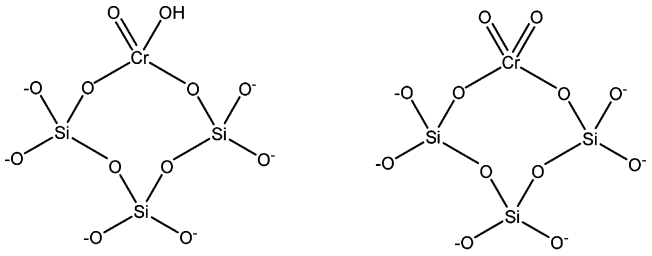

(a) (b)

O_2 complex. At elevated temperature, electron transfer occurs between Cr^{5+} and O_2 to form $Cr^{6+}-O_2^-$. After evacuation at elevated temperature, an electron transfers back to Cr^{6+} to release O_2 and form tetrahedral Cr^{5+}.[17−19] This observation shows the presence of $Cr^{6+}-O_2^-$ in the calcined CrSBA-15(*x*H) samples.

The ESR results reveal that the "efficiency" of Cr-ion incorporation increases when the n_{H_2O}/n_{HCl} molar ratio increases from 40 to 295. These results are in good agreement with literature,[17−19] where chromium is reportedly present as both Cr^{5+} and Cr^{6+} ions in calcined CrSBA-15 samples, and these ions are exclusively coordinated tetrahedrally to Si^{4+} on the silica pore walls, as shown in Scheme 1. Furthermore, ^{29}Si MAS NMR studies showed distinct signals at −111 and −110 ppm,[39] which have been assigned to Q_4 and Q_3 (silicon) sites, respectively.[40] However, the signal intensity of CrSBA-15 is much less than that of siliceous SBA-15; this observation clearly supports the stabilization of chromium ions via silanol groups (defect sites).

The above XRD, N_2 adsorption, ESR, and ^{29}Si MAS NMR results suggest successful isomorphous substitution of Cr species on the silica inner pore walls of SBA-15 by the pH-adjusting method. The incorporation of Cr-ion into SBA-15 under retained structural and textural order with increasing n_{H_2O}/n_{HCl} ratio can be explained by the synthesis mechanism of SBA-15 proposed by Zhao et al.[3] According to this mechanism (eq 1), the formation of hexagonal mesophase under highly acidic conditions occurs through the $S^0H^+X^-I^+$ pathway (nonionic polymeric surfactant (S^+), halogen anions/counter anions (X^-), and the protonated inorganic SiO_2 species (I^+). Under highly acidic synthesis medium (pH < 2), the alkylene oxide groups of the surfactant are clearly solubilized, and the hydronium ions are then associated with the alkylene oxide units while the silica species are positively charged by diluting hydrochloric acid solution. The charge-associated alkylene oxide units and the cationic silica species are equally assembled together by a combination of electrostatic, hydrogen bonding, and van der Waals interactions $REO_{m-y}[(EO)\cdot H_3O^+]_y\cdots yX^-\cdots I^+$, which can be designated as $(S^0H^+)(X^-I^+)$. As already mentioned above, under highly acidic condition, the introduction of Cr is very difficult due to the high solubility of the Cr precursors. This can be explained by the following equations:

$$Cr(NO_3)_{3(s)} + 3H^+_{(aq)} \rightleftharpoons Cr^{3+}_{(aq)} + 3HNO_{3\,(aq)}\ (pH < 1.6) \quad (1)$$

$$Cr^{3+} + 2H_2O \rightarrow Cr(OH)_2^+ + 2H^+\ (pH > 2) \quad (2)$$

For the synthesis of purely siliceous SBA-15, the above mechanism clearly shows that a highly acidic medium is necessary for the formation of the hexagonal mesophase SBA-15 but prohibits the introduction of chromium. Hence, to optimize the incorporation of Cr in the framework of SBA-15, the pH of the synthesis medium has been optimized in this study by adjusting the n_{H_2O}/n_{HCl} ratio. Initially, the formation of the hexagonal phase has been investigated by adjusting the pH of the synthesis gel between 0 and 1.7. Once the surfactant and silica species are protonated, the cationic silica species undergo partial condensation and form mesostructure through the interaction of counter anions (X^-) with the cationic surfactant species; as a result, the pH of the synthesis medium increases. It should be noted that when the n_{H_2O}/n_{HCl} ratio is increased from 40 to 166, the pH of the synthesis gel still reaches 1.8 (i.e., the synthesis gel is still very acidic) even after the addition of the silicon source and a few hours of stirring. However, by increasing the n_{H_2O}/n_{HCl} ratio to 295, the pH of the synthesis gel is around 2.3, which is above the zero net charge of silica. If the pH of the synthesis medium rises above the zero net charge of silica, the silica species are negatively charged, which enhances the interaction with the $Cr(OH)_2^+$ species. With decreasing H^+ concentration in the synthesis gel, the concentration of chromium hydroxyl species increases (eq 2). Hence, under lesser concentration of H^+ in the synthesis gel at a pH around 2.3, not only the partially condensed silica species are able to form Cr−O−Si bond with $Cr(OH)_2^+$ species but also the structural and textural order of the mesoporous framework can still be maintained. This result shows that the incorporation of heteroatom on SBA-15 silica walls depends on the concentration of H^+ ions.

Effect of Chromium Sources. To investigate the effect of the nature of Cr-ion sources, CN, CC, and CS have been used in this study as the Cr sources for the synthesis of CrSBA-15. There is a small variation in the n_{Si}/n_{Cr} ratio of the calcined CrSBA-15 as a function of the Cr source used in the synthesis gel with a fixed n_{H_2O}/n_{HCl} molar ratio of 295.

(39) Sakthivel, A.; Badamali, S. K.; Selvam, P. *Catal. Lett.* **1996**, *102*, 141.
(40) Stocker, M. *Stud. Surf. Sci. Catal.* **1996**, *102*, 141.

Table 2. Structural and Textural Parameters of CrSBA-15 Materials Prepared by Using Different Chromium Sources

sample	n_{H_2O}/n_{HCl}	n_{Si}/n_{Cr} ratio		Cr (wt %)	d_{100} (Å)	a_o (Å)	A_{BET} (m^2/g)	d_p (Å)	V_p (cm^3/g)	$t_w = a_o - d_p$ (Å)
		gel	calcined							
CrSBA-15(CS)	295	6	11.32	0.384	99.0	114.3	850	82.8	1.06	31.5
CrSBA-15(CC)	295	6	9.8	0.443	105.1	121.3	970	88.4	1.10	32.9
CrSBA-15(CN)	295	6	9.6	0.452	111.2	128.4	987	89.4	1.10	39.0

Based on the ICP-AES measurements (Table 2), the n_{Si}/n_{Cr} ratios of the calcined CrSBA-15 materials starting from a n_{Si}/n_{Cr} ratio of 6 in the synthesis gel are 9.6 (CrSBA-15(CN)), 9.8 (CrSBA-15(CC)), and 11.32 (CrSBA-15(CS)). CrSBA-15(CN) and CrSBA-15(CC) show a very high amount of Cr-ion incorporation. This is in agreement with the synthesis of CrMCM-41, showing that the use of CN and CC facilitates the incorporation of the Cr-ion into the silica pore walls.[17,18] Because the use of CS slightly reduces the pH in the synthesis gel, the amount of incorporation of Cr-ion in the silica pore walls slightly decreases. As reported above, generally a highly acidic synthesis gel is not favorable for heteroatom incorporation; thus, as compared to CrSBA-15(CN) and CrSBA-15(CC), which were synthesized using a different Cr source, incorporation of Cr species in CrSBA-15(CS) slightly decreases because the synthesis gel may become highly acidic (pH < 2).

Figure 2S shows the powder XRD patterns of CrSBA-15 prepared using CN, CC, and CS. The materials prepared from different Cr sources show the well-resolved XRD peaks, which are indexed to the (100), (110), (200), (210), and (300) reflections of the hexagonal space group *p6mm*. The intensity of the XRD patterns for CrSBA-15(CN) and CrSBA-15(CC) is higher than that observed for CrSBA-15(CS). Furthermore, using various Cr sources, the intensities of the XRD reflection and structural properties (Table 2) could be varied with respect to their counterions (such as NO_3^-, Cl^-, and SO_4^{2-}) because the counterions would affect the interaction of the surfactant with the silicate species. This observation is explained as follows. The nitrate ion especially gives the strongest counterion association, which neutralizes the micellar charge. The stronger charge neutralization would in turn help the formation of more rigid micelles and hence better hexagonal structure along with short synthesis time.[41,42] Thus, the intensity of the XRD pattern of CrSBA-15(CN) is higher as compared to those of CrSBA-15(CS) and CrSBA-15(CC). Furthermore, the divalent sulfate ion from the CS source shows somewhat different behavior as it creates HSO_4^- species in the synthesis medium. Because the HSO_4^- species bind only weakly with the cationic surfactant, the formation of $(S^0H^+)(X^-I^+)$ is much inhibited. Although, with increasing the molar ratio of n_{HCl}/n_{HCl} ratios from 40 to 295, Cr species content increases due to the decrease of H^+ concentration. Thus, the unit cell parameter of the resulting mesoporous materials increases in this order: CrSBA-15(CN) < CrSBA-15(CC) < CrSBA-15(CS). Therefore, CrSBA-15(CS) has the lowest intensity of the XRD pattern and the lowest unit cell constant as compared to CrSBA-15(CN) and CrSBA-15(CC).

Figure 4A shows the nitrogen adsorption isotherms of CrSBA-15 samples prepared using different Cr sources, and the textural parameters of the resulting samples are summarized in Table 2. All samples exhibit a higher degree of structural ordering, as indicated by the capillary condensation step of the respective adsorption isotherm. The specific surface areas of CrSBA-15(CN), CrSBA-15(CC), and CrSBA-15(CS) are 987, 970, and 850 m^2/g, respectively. CrSBA-15(CN) and CrSBA-15(CC) samples possess similar specific pore volumes of 1.10 cm^3/g, while their pore diameter is determined to be 89.4 and 88.4 Å (Figure 4B), and their pore wall thickness is calculated to be 39 and 32.9 Å, respectively. Moreover, the textural parameter values of CrSBA-15(CN) and CrSBA-15(CC) are significantly higher than those of CrSBA-15(CS) and the parent material SBA-15. It is interesting to note that the unit cell parameter, pore diameter, and pore wall thickness of CrSBA-15(CN) are

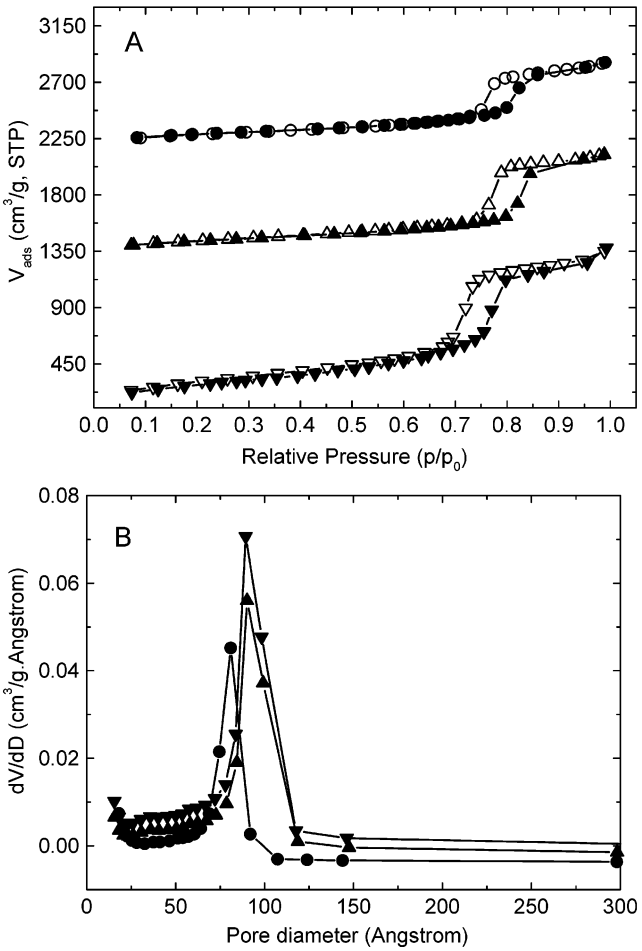

Figure 4. (A) Nitrogen adsorption isotherms of CrSBA-15 materials prepared at different chromium sources (closed symbols, adsorption; open symbols, desorption): (▼) CrSBA-15(CN), (▲) CrSBA-15(CC), and (●) CrSBA-15(CS). (B) BJH pore size distributions for CrSBA-15 materials prepared at different chromium sources: (▼) CrSBA-15(CN), (▲) CrSBA-15(CC), and (●) CrSBA-15(CS).

(41) Evans, D. F.; Wennerstrom, H. *The Colloid Domain*; VCH: New York, 1994.
(42) Israelachvili, J. N.; Mitchell, D. J.; Ninham, B. W. *J. Chem. Soc., Faraday Trans. B* **1976**, *72*, 1525.

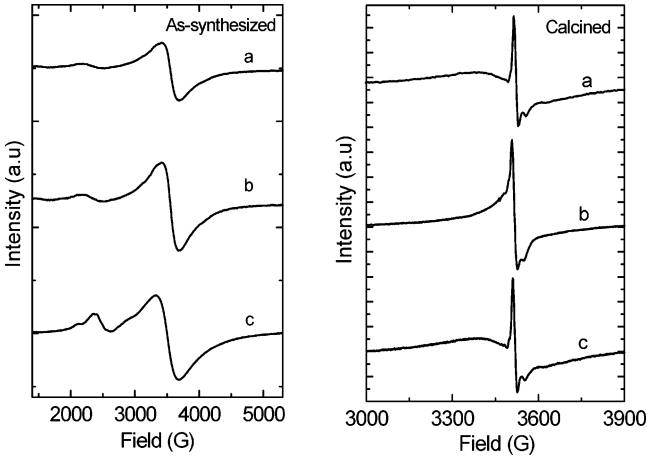

Figure 5. ESR spectra of CrSBA-15 materials prepared at different chromium sources: (a) CrSBA-15(CS), (b) CrSBA-15(CN), and (c) CrSBA-15(CC).

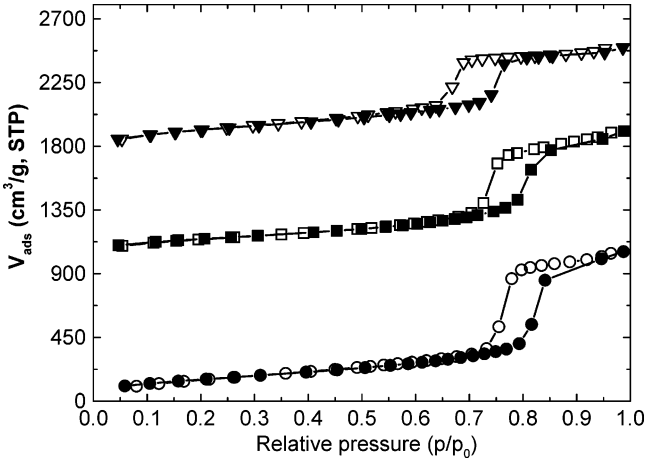

Figure 6. Nitrogen adsorption isotherms of CrSBA-15 materials prepared at different n_{Si}/n_{Cr} ratios (closed symbols, adsorption; open symbols, desorption): (●) CrSBA-15(4), (■) CrSBA-15(25), and (▼) CrSBA-15(50).

larger than those of CrSBA-15(CS). It has been reported that the charge/radius (Z/r, Å^{-1}) ratio of the central cation of the anionic species controls the rate of the silica condensation.[43] It is also found that the time required for obtaining a well-ordered MCM-41 material decreases with increasing Z/r ratio. The Z/r ratio of NO_3^- may be 2 times higher than that of SO_4^{2-}, and hence NO_3^- ion promotes more silica condensation and helps the formation of a thicker wall of the hexagonal structure in the SBA-15 materials. All of these observations indicate that the structural order, textural parameters, and the incorporation of chromium-ion in CrSBA-15 materials can be achieved using different sources of chromium.

The ESR spectra of as-synthesized and calcined CrSBA-15(CN), CrSBA-15(CC), and CrSBA-15(CS) samples are shown in Figure 5. It can be seen that the chromium source influences both the extent of Cr incorporation and its coordination in the SBA-15 pore walls. The ESR intensities of both as-synthesized and calcined CrSBA-15(CN) and CrSBA-15(CC) are higher than that of CrSBA-15(CS) due to the higher incorporation of Cr-ions in the silica walls. The ESR spectra of as-synthesized CrSBA-15 (CN), CrSBA-15(CS), and CrSBA-15(CC) samples show the g^A values are around at 1.98−2.05, indicating that Cr^{3+} is octahedrally coordinated to tetrahedral Si^{4+} in the silica pore walls. After calcination, the Cr^{3+} signal in all samples disappears, while O_2^- radical for the corresponding samples appears with g_1^B values around at 1.97−2.04, and g_2^B values around at 1.96−2.03 (Figure 5). Although there is an increase in the intensity of O_2^- radical with a high Cr-ion content, this O_2^- radical signal is not observed in all calcined siliceous SBA-15 samples. The g_3^B value of the O_2^- radical is strongly dependent on the positive charge of the nearest cation.[38] The fact that the intensity of O_2^- radical in CrSBA-15(CN), CrSBA-15(CS), and CrSBA-15(CC) samples increases linearly with Cr-ion content and that the g_2^B values are around at 1.98−2.03 indicates that O_2^- radical is connected with tetrahedral Cr^{6+} to form $Cr^{6+}-O_2^-$. Based on the ESR spectra characterizing the interaction of tetrahedral Cr^{5+}, the $Cr^{6+}-O_2^-$ interaction in calcined CrSBA-15 is postulated to be produced as follows. During the calcination of all CrSBA-15 samples, Cr^{3+} is oxidized to tetrahedral Cr^{5+}, which then coordinates with one molecule of O_2 to form a five-coordinated square-pyramidal $Cr^{5+}-O_2$ complex. At elevated temperature, electron transfer occurs between Cr(V) and O_2 to form Cr(VI)$-O_2^-$, resulting in both Cr^{5+} and Cr^{6+} to be tetrahedrally coordinated to the silica pore walls (Scheme 1).

Effect of n_{Si}/n_{Cr} Ratios. For the analysis of elemental compositions, calcined CrSBA-15 materials synthesized using Cr(III) nitrate as the Cr source with different n_{Si}/n_{Cr} ratios are characterized by ICP-AES, and the results are listed in Table 3. Generally, in all cases, the n_{Si}/n_{Cr} ratios of the calcined materials are lower than n_{Si}/n_{Cr} ratios in the synthesis gel because the materials could be synthesized under acidic conditions; however, in this condition, Cr precursors are highly dissociated. In this synthesis method, the n_{Si}/n_{Cr} ratio decreases from 99.8 to 9.1 due to the higher Cr incorporation on the silica pore walls by the formation of more Cr hydroxyl groups.

Figure 3S shows the powder XRD patterns of CrSBA-15 samples with different n_{Si}/n_{Cr} ratios. All samples show at least four well-resolved peaks, which are indexed to the (100), (110), (200), and (210) reflections. Because the XRD peaks shift to lower angle with increasing Cr-content, an increase in the *d*-spacing values and unit cell parameters is observed as compared to the purely siliceous SBA-15. The expansion in the unit cell dimension with decreasing Si/Cr ratio could be attributed to the larger radius of Cr^{5+} than that of Si^{4+}, and/or the longer Cr−O bond distance as compared to the Si−O bond distance. Therefore, these results show that the mesostructural order could not be affected by the presence of pentavalent chromium ions in the framework structure of SBA-15.

Figure 6 shows the nitrogen adsorption isotherms of calcined CrSBA-15 samples prepared with different n_{Si}/n_{Cr} ratios. All isotherms show a sharp condensation step at relative pressures in the range of 0.63−0.91. It can also be seen that the capillary condensation step is shifted to higher relative pressures with increasing chromium content in the calcined samples, resulting in the increase of pore diameter

(43) Laha, S. C.; Kumar, R. *Microporous Mesoporous Mater.* **2002**, *53*, 163.

Table 3. Structural and Textural Parameters of CrSBA-15 Materials Prepared at Different n_{Si}/n_{Cr} Ratios

sample	n_{H_2O}/n_{HCl}	n_{Si}/n_{Cr} ratio gel	n_{Si}/n_{Cr} ratio calcined	Cr (wt %)	d_{100} (Å)	a_o (Å)	A_{BET} (m^2/g)	d_p (Å)	V_p (cm^3/g)	$t_w = a_o - d_p$ (Å)
CrSBA-15(4)	295	4	9.1	0.477	112.3	129.7	973	89.5	1.11	40.2
CrSBA-15(16)	295	16	17.3	0.251	106.3	122.7	1015	88.5	1.09	34.2
CrSBA-15(25)	295	25	52.1	0.083	102.6	118.5	1037	87.2	1.08	31.3
CrSBA-15(50)	295	50	99.8	0.043	99.2	114.5	1063	86.5	1.09	28.0

with the increase of Cr content in the sample. Moreover, with the decrease of n_{Si}/n_{Cr} ratio in the calcined sample, the pore diameter, pore volume, and pore wall thickness increase with the decrease of the specific surface area (Table 3). The unit cell size also increases monotonically with the decrease of n_{Si}/n_{Cr} ratio of the calcined samples. The same effect has been found when CN was used as the Cr source in the synthesis of MCM-41.[17,19] It is obvious that the enlargement of the unit cell size is not a consequence of Cr incorporation into the pore walls because the enlargement of the unit cell size is limited to the use of Cr(III) nitrate as the Cr source. The observed enlargement of pore size in CrSBA-15(CN) could be explained as follows. In crystalline zeolites, their pore size slightly increase with incorporation of metal-ions because of the longer bonding length of metal ion with oxygen than the Si−O bond length. However, there is no such rule for SBA-15 as it has an amorphous structure where both bond length and bond angle may change. It has been usually observed that the pore size of SBA-15 decreases after the incorporation of metal-ions, but so far there has been no clear explanation for this observation. Although SBA-15 has thicker pore walls relative to zeolites, not all metal-ions can be incorporated or substituted into the silica framework completely. This is because some of these metal-ions may be exposed on the pore wall surface, behaving as impregnated metal-ion complexes on the pore walls of SBA-15. These metal-ions may then interact with surface hydroxyl groups and may contract the pore wall when combined with two or three hydroxyl groups, causing the pore size to decrease.[44,45] However, if these metal-ions are incorporated deeply within the silica framework, this pore shrinkage might not occur as the metal ions could not interact with the surface hydroxyl groups, and the pore size might be increased instead by the increase of metal−oxygen bond length, which has been similarly observed for zeolites. According to the above hypothesis, this unusual result strongly suggests that Cr-ions have been incorporated into the silica framework. Moreover, the enlargement of pore size occurs without any ascertainable change in the structural order of the mesoporous materials with increasing amount of CN in the synthesis gel. In addition, all CrSBA-15 materials prepared with various n_{Si}/n_{Cr} ratios from 99.8 to 9.1 possess higher pore volumes than purely siliceous SBA-15 materials, possibly indicating the presence of a high fraction of ultra-micropores in CrSBA-15 samples. All of these results suggest that CrSBA-15 materials can be prepared with very high chromium content ($n_{Si}/n_{Cr} = 9.1$) without affecting the structural order of the resulting mesoporous materials.

The ESR spectra of calcined CrSBA-15(4) and CrSBA-15(50) are shown in Figure 7. The ESR intensity generally increases with decreasing molar ratio of n_{Si}/n_{Cr} because the Q_3 silanol groups interact strongly with Cr-ions. Because CrSBA-15(4) has higher ESR intensity than CrSBA-15(50), there is a greater Cr-ion incorporation in CrSBA-15(4) than CrSBA-15(50). The Cr^{5+} and Cr^{6+} species in different molar n_{Si}/n_{Cr} ratios of CrSBA-15 samples are tetrahedrally coordinated to Si^{4+} on the silica walls. A similar behavior has also been reported for CrMCM-41 materials.[17−19]

Figure 8 shows several representative field emission-scanning electron microscopy (FE-SEM) images for mesoporous CrSBA-15(4). The morphology of CrSBA-15(4) can be controlled by the simple adjustment of the molar n_{H_2O}/n_{HCl} ratio in the synthesis gel at a fixed n_{Si}/n_{Cr} ratio to 4, with the resulting morphology as ropelike hexagonal mesoporous materials. CrSBA-15 material is made up of a bundle of ropes of diameter ~12 μm and with a long ropelike aspect of as much as several hundred micrometers. It should be noted that the images in Figure 10 are similar to those reported by Zhao et al.[3,4]

Figure 9 shows the TEM images of the CrSBA-15(4) sample. The TEM images show well-ordered hexagonal arrays of 1D mesoporous channels, further confirming that CrSBA-15 sample has a 2D *p6mm* hexagonal structure. The distance between two consecutive centers of hexagonal pores estimated from the TEM image is ca. ~12 nm. The average thickness of the wall is ca. ~4.0 nm, which is much larger than that for MCM-41, and the pore diameter is around ~8.9 nm, which is in agreement with the N_2 adsorption measurements.

Effect of Synthesis Temperature. Zhao et al.[11,12] reported that the unit cell size and pore diameter of SBA-15 materials increase when the synthesis temperature is varied from 383 to 403 K. In our work, the synthesis of CrSBA-15 was also conducted with the same range of synthesis temperature to

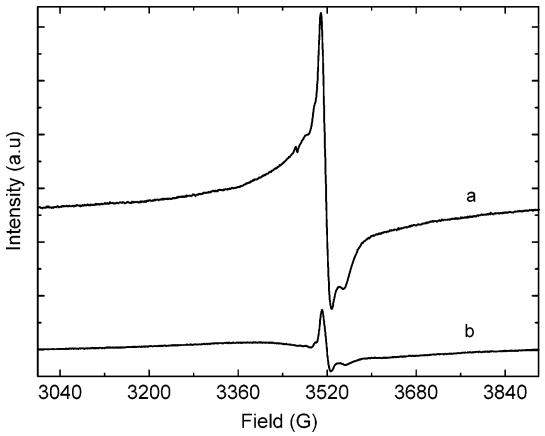

Figure 7. ESR spectra of calcined CrSBA-15 materials prepared at different n_{Si}/n_{Cr} ratios: (a) CrSBA-15(4), and (b) CrSBA-15(50).

(44) Pauly, T. R.; Liu, Y.; Pinnavaia, T. J.; Billinge, S. J. L.; Rieler, P. *J. Am. Chem. Soc.* **1992**, *121*, 8835.
(45) Morey, M.; Davidson, A.; Eckert, H.; Stucky, G. *Chem. Mater.* **1996**, *8*, 486.

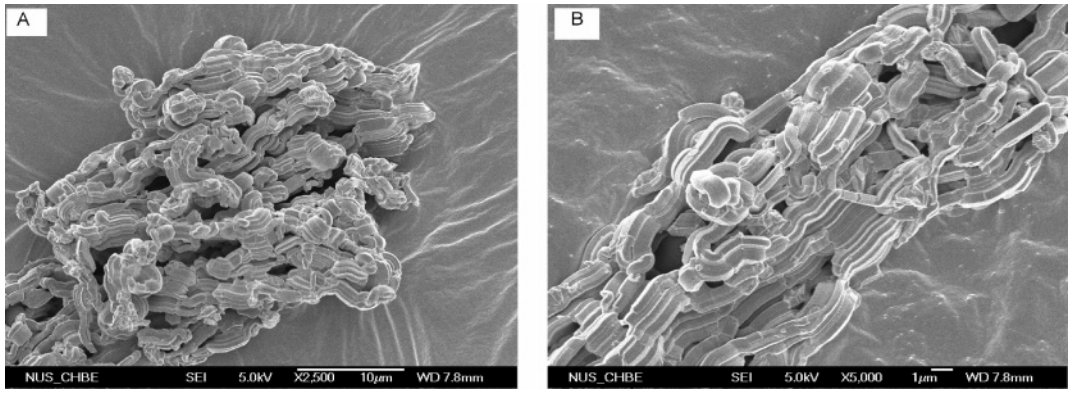

Figure 8. Micrographs of calcined hexagonal mesoporous CrSBA-15(4) obtained on a JEOL JSM-6700F microscope at different magnifications.

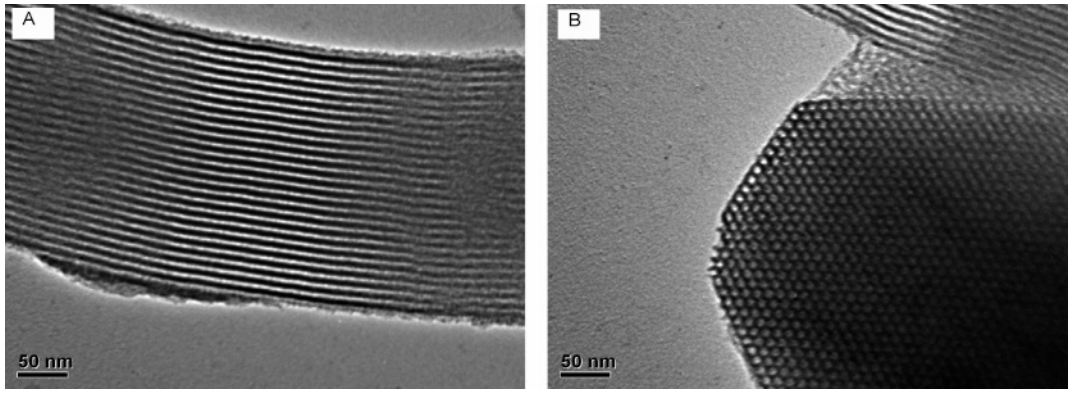

Figure 9. TEM micrographs of calcined hexagonal mesoporous CrSBA-15(4) obtained on a JEOL 2010 electron microscope.

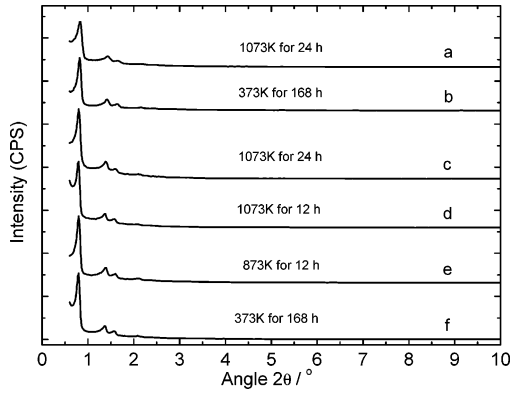

Figure 10. XRD powder patterns of CrSBA-15 materials prepared after hydrothermal treatment using boiling water and water steam: (a, b) CrSBA-15(50), and (c−f) CrSBA-15(8).

investigate their structural and textural properties. The XRD powder patterns of the calcined CrSBA-15 materials are well-defined and characteristic of well-ordered hexagonal materials (Figure 4S). However, the XRD reflection peaks are seriously shifted to lower 2θ values when the synthesis temperature is systematically increased from 373 to 403 K, resulting in the increase of the unit cell size (Table 4). Moreover, at higher synthesis temperature (403 K), the strong intensity of all reflection peaks in CrSBA-15(403K) indicates that the material possesses thinner walls as suggested by Zhao et al.[3,4] for the analogous hexagonal structure of pure silica SBA-15. It is interesting to note that the structural orders of CrSBA-15 materials are maintained up to the synthesis temperature of 403 K. The ICP-AES results characterizing the n_{Si}/n_{Cr} ratios of all CrSBA-15 samples prepared at different synthesis temperatures show that the incorporation of Cr species on the silica walls could not be affected by increasing the synthesis temperature (Table 4).

The textural properties of the corresponding samples are shown in Table 4. The position of the capillary condensation step for these samples shifts to higher relative pressure when the synthesis temperature is increased from 373 to 403 K. Moreover, the amount of N_2 adsorbed also increases with the synthesis temperature (not shown). The textural properties obtained from examination of the nitrogen isotherms of CrSBA-15 prepared at different temperatures are summarized in Table 4. With increasing temperature, specific pore volume (1.10−1.20 cm^3/g) and pore diameter (89.4−94.7 Å) increase, whereas the specific surface area (987−797 m^2/g) and pore wall thickness (38.0−36.7 Å) decrease. The XRD and N_2-adsorption results show that there is an increase of pore diameter and unit cell parameter and a decrease of surface areas and pore wall thickness with the increase of crystallization temperature. These results may be explained on the basis of the nature of the copolymer blocks, which can be changed with different synthesis temperature.

In natural copolymer, poly(ethylene oxide) (PEO) blocks are hydrophilic and poly(propylene oxide) (PPO) blocks are hydrophobic. Under acidic hydrothermal synthesis conditions, the size of copolymer systematically increases with the gradual increase of synthesis temperature from 373 to 403 K. For the formation of the large pore of CrSBA-15, because copolymer interacts with the silanol groups via hydrogen bonds, the silanol groups then interact with Cr species by adjusting the water to hydrochloric acid ratios. The increase of copolymer size could be explained by the following reasons: at higher reaction temperatures, the length

Table 4. Structural and Textural Parameters of CrSBA-15 Materials Prepared at Different Synthesis Temperatures

sample	n_{H_2O}/n_{HCl}	n_{Si}/n_{Cr} ratio gel	n_{Si}/n_{Cr} ratio calcined	Cr (wt %)	T_{Syn} (K)	a_o (Å)	A_{BET} (m^2/g)	d_p (Å)	V_p (cm^3/g)	$t_w = a_o - d_p$ (Å)
CrSBA-15(373K)	295	8	9.9	0.439	373	127.4	987	89.4	1.10	38.0
CrSBA-15(383K)	295	8	10.0	0.435	383	128.9	957	91.0	1.11	37.9
CrSBA-15(393K)	295	8	10.0	0.435	393	130.7	848	93.3	1.13	37.4
CrSBA-15(403K)	295	8	10.0	0.435	403	131.4	797	94.7	1.20	36.7

Table 5. Structural and Textural Parameters of CrSBA-15 Materials Prepared after Hydrothermal Treatment Using Boiling Water and Water Steam

sample	hydrothermal temp (K)	hydrothermal time (h)	n_{Si}/n_{Cr} ratio gel	n_{Si}/n_{Cr} ratio calcined	Cr (wt %)	a_o (Å)	A_{BET} (m^2/g)	d_p (Å)	V_p (cm^3/g)	$t_w = a_o - d_p$ (Å)
CrSBA-15(8)	373	168	8	9.9	0.439	127.4	986	89.4	1.10	38.0
CrSBA-15(8)	873	12	8	9.9	0.439	127.3	985	89.4	1.10	37.9
CrSBA-15(8)	1073	12	8	10.0	0.435	127.2	980	89.4	1.10	37.8
CrSBA-15(8)	1073	24	8	10.0	0.435	127.2	978	89.4	1.10	37.8
CrSBA-15(50)	373	168	50	99.8	0.0436	112.2	957	85.2	1.06	27.0
CrSBA-15(50)	1073	24	50	99.9	0.0435	110.1	852	85.1	1.05	25.0

of hydrophobic part of copolymer increases by interacting more hydrophilic PEO blocks with hydrophobic PPO blocks. Hence, the hydrophilicity of PEO blocks decreases and becomes more hydrophobic than PPO at higher synthesis temperature (403 K). In the present conditions, the PEO blocks are expected to interact more closely with inorganic walls than the more hydrophobic PPO blocks. Hence, it is believed that PEO blocks are responsible for the formation of micropores in the SBA-15 framework.[3,4] The variation of copolymer size with increasing temperature from 373 to 403 K is also reflected by a substantial broadening of the pore size distribution of CrSBA-15 materials (figure not shown).

Hydrothermal Stability. To evaluate the hydrothermal stability, CrSBA-15(8) and CrSBA-15(50) materials were either treated with steam at 873 K for 12 h, at 1073 K for 12 h, and at 1073 K for 24 h or treated in boiling water at 373 K for 168 h. The distinct structural parameters are helpful for better understanding of the factors that affect the hydrothermal stability of CrSBA-15 materials because CrSBA-15 materials can be used as catalysts for the synthesis of bulk aromatic molecules in chemical industries.

Figure 10 shows the XRD patterns of CrSBA-15 samples after being treated in boiling water at 373 K for 168 h or with steam at 873 K for 12 h, at 1073 K for 12 h, and at 1073 K for 24 h. Table 5 shows that, after hydrothermal treatment of CrSBA-15(50), its (100) diffraction peak shifts to higher 2θ degree, the relative intensity of its diffraction peaks decreases, and its (300) diffraction peak disappears. Because of the low amount of Cr-ion incorporation in CrSBA-15(50), its unit cell parameter also decreases after hydrothermal treatment because it has a high number of free Si−O−Si bonds. These results suggest that the hydrothermal treatment for CrSBA-15(50) may cause somewhat shrinkage of mesopores and structural disorder. Nevertheless, CrSBA-15(50) still displays three strong and well-resolved (100), (110), and (200) diffraction peaks of *P*6*mm* symmetry, suggesting a highly ordered mesostructure.[46] However, after hydrothermal treatment of CrSBA-15(8) at different temperatures under various treatment times, its unit cell parameter remains constant because it has a high number of Si−O−Cr bonds, which are relatively stable to further attack by stream and boiling water.

The remarkable improvement of hydrothermal stability of CrSBA-15(8) due to the higher chromium-ion incorporation is further evidenced by the N_2 adsorption measurements (Table 5) on all CrSBA-15 materials after they had been treated either with steam at different temperatures under various times or with boiling water for 168 h. After hydrothermal treatment, the surface area, pore diameter, pore volume, and pore wall thickness of CrSBA-15(50) decrease, but those of CrSBA-15(8) remain almost constant. Because CrSBA-15(8) has a much higher amount of Cr-ions in the framework of silica pore walls,[47] it has more Si−O−Cr bonds that are relatively stable to further attack from boiling water. Furthermore, CrSBA-15(8) has more tetrahedral Cr^{6+}/Cr^{5+} ions, which can create more negative charge on the surface of pore walls to repel OH^- ions, and hence prevent the hydrolysis of siloxane bonds, but also can result in an increase in the number of acid sites. Because Cr is irreversibly incorporated into the structure of CrSBA-15(8), CrSBA-15(8) has higher hydrothermal stability than CrSBA-15(50). These results also further confirm that the pore wall of CrSBA-15(8) becomes thicker due to the presence of more tetrahedral Cr^{6+}/Cr^{5+} ions incorporated in the framework of silica walls, and the thick pore wall of CrSBA-15(8) displays remarkable hydrothermal stability in steam at 1073 K for 24 h. Figure 11 shows the preservation of the hexagonal ropelike morphology of CrSBA-15(8) even after steam treatment at 1073 K for 24 h, further confirming that CrSBA-14(8) has an excellent hydrothermal stability with well-ordered hexagonal morphology.

Conclusions

A new synthesis method has been developed to incorporate Cr-ions into the SBA-15 silica matrix with very high mesostructural order and high chromium content by simply adjusting the molar water to hydrochloric acid ratios in the gel mixture. ICP-AES results show that the amount of Cr

(46) Zhang, F.; Yan, Y.; Yang, H.; Meng, Y.; Yu, C.; Tu, B.; Zhao, D. *J. Phys. Chem. B* **2005**, *109*, 8723.

(47) Han, Y.; Li, N.; Zhao, L.; Li, D.; Xu, X.; Wu, S.; Di, Y.; Li, C.; Zou, Y.; Yu, Y.; Xiao, F. S. *J. Phys. Chem. B* **2003**, *107*, 7551.

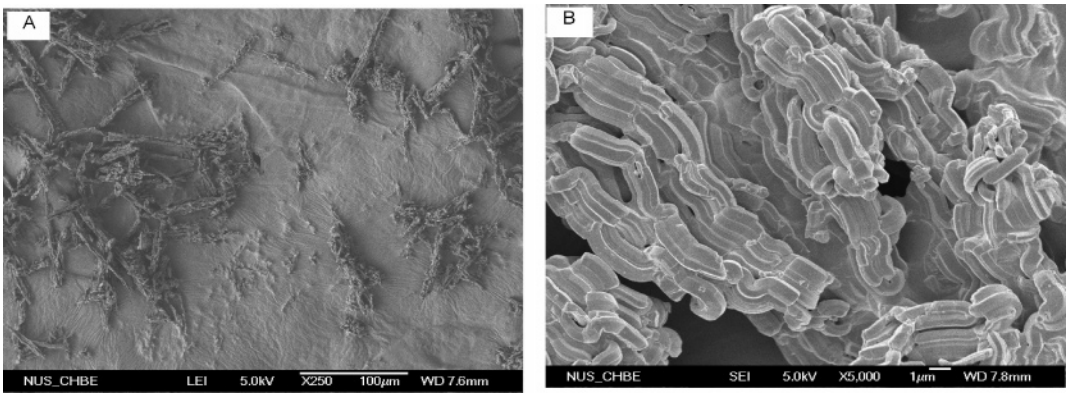

Figure 11. Micrographs of hexagonal mesoporous CrSBA-15(8) obtained after hydrothermal treatment at 1073 K on a JEOL JSM-6700F microscope at different magnifications.

species incorporated into SBA-15 prepared under a n_{H_2O}/n_{HCl} molar ratio of 295 is higher than that prepared under other n_{H_2O}/n_{HCl} molar ratios, and the n_{Si}/n_{Cr} ratios in CrSBA-15 could not be affected when the crystallization temperature is increased from 373 to 403 K. XRD and N_2 adsorption studies show that the structural and textural properties of CrSBA-15 could be affected by the Cr incorporation on the silica walls, while the unit cell dimension and pore size of CrSBA-15 can be increased by simply adjusting the crystallization temperature without addition of any organic swelling agents. ESR and ^{29}Si MAS NMR studies confirm that Cr(III) nitrate is a good Cr source among all Cr sources studied, resulting in a higher amount of Cr^{5+} species incorporated with tetrahedral coordination. FE-SEM and TEM studies confirm that CrSBA-15 samples have a long ropelike morphology and uniform pore diameter. Furthermore, the hydrothermal stabilities of hexagonal CrSBA-15 materials have been studied using stream/boiling water at different treatment temperatures with various times. The result shows that CrSBA-15(8) has superior hydrothermal stability to that of CrSBA-15(50).

Acknowledgment. The Singapore Millennium Fellowship (SMF) awarded by the Singapore Millennium Foundation to M.S. (2005-SMF-0437) is gratefully acknowledged.

Supporting Information Available: The BJH pore size distributions of CrSBA-15 materials prepared at different n_{H_2O}/n_{HCl} ratios; XRD powder patterns of CrSBA-15 materials prepared using different Cr sources, n_{Si}/n_{Cr} ratios, and temperatures. This material is available free of charge via the Internet at http://pubs.acs.org.

CM062009R